Anthropogenic influence on the 2018 summer warm spell in Europe: the impact of different spatio-temporal scales

Nicholas Leach[1]*, Sihan Li[2,3], Sarah Sparrow[2], Geert Jan van Oldenborgh[4], Fraser C. Lott[5], Antje Weisheimer[1,6,7], Myles R. Allen[1,3],

[1]Department of Physics, Atmospheric Oceanic and Planetary Physics, University of Oxford, United Kingdom.

[2]Oxford e-Research Centre, Department of Engineering Science, University of Oxford, United Kingdom.

[3]Environmental Change Institute, School of Geography and the Environment, University of Oxford, United Kingdom.

[4]Koninklijk Nederlands Meteorologisch Instituut, De Bilt, The Netherlands.

[5]UK Met Office Hadley Centre, Exeter, United Kingdom.

[6]Department of Physics, National Centre for Atmospheric Science (NCAS), University of Oxford, United Kingdom.

[7]European Centre for Medium-Range Weather Forecasts (ECMWF), Reading, United Kingdom.

*Corresponding author email: Nicholas.leach@stx.ox.ac.uk

Abstract

We demonstrate that in attribution studies, events defined over longer timescales generally produce higher probability ratios due to lower interannual variability, reconciling seemingly inconsistent attribution results of Europe's 2018 summer heatwaves in reported studies.

Introduction

The summer of 2018 was extremely warm in parts of Europe, particularly Scandinavia, the Iberian Peninsula, and Central Europe, with a range of all-time temperature records set across the continent (Johnston, 2018; NESDIS, 2018). Impacts were felt across Europe, with wildfires burning in Sweden (Krikken, Lehner, Haustein, Drobyshev, & van Oldenborgh, 2019; Watts, 2018), heatstroke deaths in Spain (Publico, 2018), and widespread drought (Harris, 2018). During the summer, the World Weather Attribution (WWA) initiative released an analysis of the heat-spell (World Weather Attribution, 2018) based on observations/forecasts and models in specific locations (Dublin, Ireland; De Bilt, Netherlands; Copenhagen, Denmark; Oslo, Norway; Linkoping, Sweden; Sodankyla, Finland; Jokionen, Finland), which concluded that the increase in likelihood due to human-induced climate change was at least two to five times. In December, the UK Met Office (UKMO) stated that they found the 2018 UK summer temperatures were made thirty times more likely (Press Office, 2018; McCarthy, et al., 2019). These two estimates appear to quantitatively disagree, however we show they can be reconciled by investigating the effects of using different spatial domains and temporal scales in the event definition. We also demonstrate that prescribed SST model simulations can underrepresent the variability of temperature extremes, especially near the coast, with implications for any derived attribution results.

Event Definition

We consider various temperature-based event definitions to demonstrate the impact of this choice in attribution assessments, and assess to what extent human influence affected the seasonal and peak magnitudes of the 2018 summer heat-event on a range of spatial scales. The statistic we use is the annual maximum of the 1, 10 and 90 day running mean of daily mean 2m temperature, (hereafter TM1x, TM10x and TM90x respectively). We analyse three spatial scales: model gridbox, regional and European. For regional and European event definitions, the spatial mean is calculated before the running mean. Regional extents are taken from Christensen and Christensen (2007), and European extent is the E-OBS (Cornes, van der Schrier, van den Besselaar, & Jones, 2018) domain [land points in 25N-71.5N, 25W-45E]. The WWA used the annual maxima of 3-day mean daily maximum temperatures at specific gridpoints for its connection to local health effects (D'Ippoliti, et al., 2010), while the UKMO used the JJA mean temperature over the entire UK in order to answer the question of how anthropogenic forcings have affected the likelihood of UK summers as warm as 2018. The same justifications can be used here, though we add that different heat-event timescales are important to different groups of people, and as such using several temporal definitions may increase interest in heat-event attribution studies. However, we recognise that other definitions than those used here may be more relevant to some impacts observed (such as defining the event in the context of the atmospheric flow pattern and drought which accompanied the heat), and other lines of reasoning for selecting one particular event definition exist (Cattiaux & Ribes, 2018).

Model Simulations and Validation

Three sets of simulations from the UKMO Hadley Centre HadGEM3-A global atmospheric model (Christidis, et al., 2013; Ciavarella, et al., 2018) are used. These are a historical ensemble (1960-2013, Historical), and factual (ACT) and counterfactual (a ``natural" world without anthropogenic forcings, NAT) ensembles of 2018. We compare results from this factual-counterfactual analysis with those from a trend-based analysis of Historical, ensembles from EURO-CORDEX (Vautard, et al., 2013; Jacob, et al., 2014; Vrac, Vaittinada Ayar, & Ayar, 2017) (1971-2018) and RACMO (Aalbers, Lenderink, van Meijgaard, & van den Hurk, 2018; Lenderink, et al., 2014) (1950-2018), and observations from E-OBS (1950-2018). A full model description is provided in the Supplementary Information. Initially, we performed our analysis with the weather@home HadRM3P European-25km setup (Massey, et al., 2015), but found this model overestimates the variability over all Europe for daily through seasonal scale event statistics and so was omitted.

Methodology

We calculate the return period, RP, for the 2018 event in a distribution fit to E-OBS using the generalised extreme value (GEV) distribution to model TM1x and TM10x, and the generalised logistic distribution to empirically model TM90x throughout. Since the distribution of temperature extremes changes as the climate does, to account for the non-stationarity of the timeseries we first remove the trend attributable to low-pass-filtered globally-averaged mean surface temperature [GMST, from Berkeley Earth (Rohde, et al., 2013)] in an ordinary-least-squares regression [the regression coefficient or trend is shown in SI Fig. 1 (Diffenbaugh, et al., 2017)]. We then find the temperature threshold corresponding to RP in a distribution fit to the model's climatology. In the factual-counterfactual analysis, we do this by fitting parameters to a detrended (against GMST, trends shown in SI Fig. 2c7-c9) climatological ensemble of Historical plus 15 randomly sampled members of ACT. We finally calculate the probability (P) of exceeding this climatological temperature threshold in distributions fit to the ACT and NAT ensembles and calculate the probability ratio, $\mathrm{PR} = P_{\mathrm{ACT}}/P_{\mathrm{NAT}}$, representing the increased likelihood of the 2018 event in the factual compared to the counterfactual world. Using estimated event probabilities rather than observed magnitudes constitutes a quantile bias correction (Jeon, Paciorek, & Wehner, 2016), minimizing model biases in the mean and variability of the temperatures analysed. A description of uncertainty calculation and the trend-based analysis discussed below is included in the SI.

Results

Extreme daily heat-events, measured by TM1x, are distributed heterogeneously throughout Europe (SI Fig. 1i). This is paralleled in the factual-counterfactual PRs seen in Fig. 1a, with large proportions of Iberia, the Netherlands, and Scandinavia experiencing events that were highly unlikely in a climate without anthropogenic influence. A similar result is found on the regional scale (Fig. 1d) with Scandinavia and the Iberian Peninsula respectively experiencing 1-in-150 [26 , 26000][1] and 1-in-30 [9 , 550] year events in the current climate that were highly unlikely in the natural climate simulated in NAT. The remaining regions record maximum daily temperatures likely to be repeated within 4 years. Considering the whole of Europe, the likelihood of the 2018 maximum of daily European mean temperature occurring without climate change is zero. This result is consistent with Uhe, et al., (2016) and Angélil,

[1] Numbers in [ ] represent a 90\% confidence interval

et al., (2018), who showed that increasing spatial scale tends to increase the probability ratio.

Extreme 10-day heat-events, TM10x, were also widespread in Europe, with the most extreme occurring in Scandinavia (SI Fig. 1j). Regionally, the PRs become more uniform (Fig. 1d), though Scandinavia and the Iberian Peninsula still have very high best-estimate PRs of 185 [17 , infinite] and 110 [18 , 56000] respectively. The best-estimate PR for the average of Europe is still formally infinite.

The PR map for season-long heat-events measured by TM90x is more uniform throughout Europe (Fig. 1c). Scandinavia, British Isles, France, and Central and Eastern Europe regions all experienced on the order of 1-in-10 year events (SI Fig. 1l), and the corresponding best-estimate PRs are between 10 and 100 for all regions (Fig. 1d), including those with lower return periods. The PR for the European average is 1000 [500 - 2000].

Trend-based analysis, SI Figs. 1m-p (observations) and 2b (models), yields similar results, though we note that for HadGEM-3A this results in generally higher PRs, due to the linear trend with GMST in the climatology being greater than the difference between the two ensembles used in the factual-counterfactual analysis. Observational and model analysis contradict in some gridboxes in Northern Scandinavia for TM1x and TM10x, since the observed best-estimate trend against GMST is negative, reducing the event probability for the present-day compared to the pre-industrial climate, therefore yielding PRs of less than 1. Comparing regional factual-counterfactual model with observational analysis (Fig. 1d vs SI Fig. 1p) shows that the large observational uncertainties overlap with the model results: the difference could be due to natural variability affecting the small observational sample size.

However, we are cautious of drawing any conclusions regarding the change in likelihood of extreme heat-events as defined here for these locations.

The PR increases with the event statistic timescale for the majority of gridpoints and regions (shown in Fig. 1). Fig. 2 illustrates the cause using the British Isles region: as the timescale increases, the event statistic distribution variance decreases, while the mean shift between the factual and counterfactual distributions remains constant. SI Fig 1t shows that the similarity in trends with GMST between the three timescales is also true for the observations. The decrease in variance usually results in higher PRs, given a particular event return time, for the longer timescales. There are exceptions due to the bounded upper tail of a GEV distribution with a negative shape parameter, resulting in the very high PRs for TM1x in Scandinavia, Iberia and the Netherlands. The solid and dotted black lines compare the temperature thresholds when using event return periods to anomaly magnitudes in E-OBS. This explains why the TM90x PR is much higher than the other timescales for the British Isles: in addition to the decreased variance, the seasonal-scale heat-event was more unusual than the other timescales, with a longer return period (10.6 [5.7 , 21] years) than TM10x (2.6 [1.8 , 3.9] years) and TM1x (3.6 [2.5 , 6.2] years). These factors together result in PRs of 3.6 [2.9 - 4.8] for TM1x and 43 [27 - 84] for TM90x. We suggest that the change in variance between the timescales used largely reconciles the differences between the ``two to five'' and ``thirty'' times increases in likelihood found by the WWA and UKMO reports, with other methodological factors playing a minor role. Although the higher return period for TM90x has some impact, it is less significant that the change in variability.

Fig. 2 also demonstrates a relevant deficiency in the model: the model distributions are narrower than the observed distributions, meaning the model has lower variability than the real world. This reduced variance has a significant impact on attribution results (Bellprat, Guemas, Doblas-Reyes, & Donat, 2019), and means that the PRs for the British Isles presented here, especially for TM90x, are likely to be overestimated. Underrepresented variability often occurs in prescribed SST models (Fischer, Beyerle, Schleussner, King, & Knutti, 2018), and is visible in HadGEM-3A for many coastal locations over Europe (SI Fig. 2a7-a9). Fig. 2d shows the power spectrum of JJA summer temperatures over the British Isles, indicating that HadGEM3-A has similar spectral characteristics to E-OBS, but underrepresents the intraseasonal 2m temperature variability at almost all frequencies, which will likely result in overestimated PRs. Power spectra for other model ensembles are shown for comparison, demonstrating that the fully bias-corrected EURO-CORDEX ensemble has the same variability characteristics and magnitude as the observations.

Discussion

Our analysis highlights a key property of extreme weather attribution: the variance of the event definition used, both in terms of the statistic itself and its representation within any models used. The use of longer temporal event scales in general increases both the spatial uniformity and magnitude of the probability ratios found, consistent with Kirchmeier-Young, Wan, Zhang, & Seneviratne (2019), due to a decrease in variance compared to shorter scales. The difference in temporal scale between two reports concerning the 2018 summer heat is sufficient to explain the large discrepancy in attribution result between them. We find that several European regions experienced season-long heat-events with a present-day return period greater than 10 years. The present-day likelihood of such events occurring is approximately 10 to 100 times greater than a ``natural" climate. The attribution results also show that the extreme daily temperatures experienced in parts of Scandinavia, the

Netherlands and Iberia would have been highly unlikely without anthropogenic warming. The prescribed SST model experiments used here tend to underestimate the variability of temperature extremes near the coast, which may lead to the attribution results overstating the increase in likelihood of such extremes due to anthropogenic climate change (Bellprat, Guemas, Doblas-Reyes, & Donat, 2019). We aim to properly quantify the impact of the underrepresented variability in further work. Although here we have used an unconditional temperature definition for consistency with the studies we try to reconcile, we plan to further investigate the effect of including both the atmospheric flow context and other impact related variables such as precipitation in the event definition, and address issues models might have with realistically simulating the physical drivers of heatwaves.

Acknowledgements

We acknowledge the E-OBS dataset from the EU-FP6 project UERRA (http://www.uerra.eu) and the Copernicus Climate Change Service, and the data providers in the ECA\&D project (https://www.ecad.eu). We would like to thank all of the volunteers who have donated their computing time to Climateprediction.net and Weather@Home.

References

Aalbers, E. E., Lenderink, G., van Meijgaard, E., & van den Hurk, B. J. (2018, jun). Local-scale changes in mean and heavy precipitation in Western Europe, climate change or internal variability? *Climate Dynamics, 50*(11-12), pp. 4745-4766.

Angélil, O., Stone, D., Perkins-Kirkpatrick, S., Alexander, L. V., Wehner, M., Shiogama, H., . . . Christidis, N. (2018, apr). On the nonlinearity of spatial scales in extreme weather attribution statements. *Climate Dynamics, 50*(7-8), pp. 2739-2752.

Bellprat, O., Guemas, V., Doblas-Reyes, F., & Donat, M. G. (2019, dec). Towards reliable extreme weather and climate event attribution. *Nature Communications, 10*(1), p. 1732.

Cattiaux, J., & Ribes, A. (2018, aug). Defining Single Extreme Weather Events in a Climate Perspective. *Bulletin of the American Meteorological Society, 99*(8), pp. 1557-1568.

Christensen, J. H., & Christensen, O. B. (2007, may). A summary of the PRUDENCE model projections of changes in European climate by the end of this century. *Climatic Change, 81*(S1), pp. 7-30.

Christidis, N., Stott, P. A., Scaife, A. A., Arribas, A., Jones, G. S., Copsey, D., . . . Tennant, W. J. (2013, may). A New HadGEM3-A-Based System for Attribution of Weather- and Climate-Related Extreme Events. *Journal of Climate, 26*(9), pp. 2756-2783.

Ciavarella, A., Christidis, N., Andrews, M., Groenendijk, M., Rostron, J., Elkington, M., . . . Stott, P. A. (2018, jun). Upgrade of the HadGEM3-A based attribution system to high resolution and a new validation framework for probabilistic event attribution. *Weather and Climate Extremes, 20*, pp. 9-32.

Cornes, R. C., van der Schrier, G., van den Besselaar, E. J., & Jones, P. D. (2018, sep). An Ensemble Version of the E-OBS Temperature and Precipitation Data Sets. *Journal of Geophysical Research: Atmospheres, 123*(17), pp. 9391-9409.

D'Ippoliti, D., Michelozzi, P., Marino, C., De'Donato, F., Menne, B., Katsouyanni, K., . . . Perucci, C. A. (2010). The impact of heat waves on mortality in 9 European cities: Results from the EuroHEAT project. *Environmental Health: A Global Access Science Source, 9*(1).

Diffenbaugh, N. S., Singh, D., Mankin, J. S., Horton, D. E., Swain, D. L., Touma, D., . . . Rajaratnam, B. (2017, may). Quantifying the influence of global warming on unprecedented extreme climate events. *Proceedings of the National Academy of Sciences of the United States of America, 114*(19), pp. 4881-4886.

Fischer, E. M., Beyerle, U., Schleussner, C. F., King, A. D., & Knutti, R. (2018, aug). Biased Estimates of Changes in Climate Extremes From Prescribed SST Simulations. *Geophysical Research Letters, 45*(16), pp. 8500-8509.

Harris, C. (2018, aug). Heat, hardship and horrible harvests: Europe's drought explained. *Euronews*. Retrieved from https://www.euronews.com/2018/08/10/explained-europe-s-devastating-drought-and-the-countries-worst-hit

Jacob, D., Petersen, J., Eggert, B., Alias, A., Christensen, O. B., Bouwer, L. M., . . . Yiou, P. (2014, apr). EURO-CORDEX: new high-resolution climate change projections for European impact research. *Regional Environmental Change, 14*(2), pp. 563-578.

Jeon, S., Paciorek, C. J., & Wehner, M. F. (2016, jun). Quantile-based bias correction and uncertainty quantification of extreme event attribution statements. *Weather and Climate Extremes, 12*, pp. 24-32.

Johnston, C. (2018, aug). Heatwave temperatures may top 45C in southern Europe. *The Guardian*. Retrieved from https://www.theguardian.com/world/2018/aug/04/temperatures-in-southern-europe-top-45-heatwave-spain-portugal

Kirchmeier-Young, M. C., Wan, H., Zhang, X., & Seneviratne, S. I. (2019, sep). Importance of framing for extreme event attribution: the role of spatial and temporal scales. *Earth's Future*.

Krikken, F., Lehner, F., Haustein, K., Drobyshev, I., & van Oldenborgh, G. J. (2019, aug). Attribution of the role of climate change in the forest fires in Sweden 2018. *Natural Hazards and Earth System Sciences Discussions*, pp. 1-24.

Lenderink, G., van den Hurk, B. J., Klein Tank, A. M., van Oldenborgh, G. J., van Meijgaard, E., de Vries, H., & Beersma, J. J. (2014, nov). Preparing local climate change scenarios for the Netherlands using resampling of climate model output. *Environmental Research Letters, 9*(11), p. 115008.

Massey, N., Jones, R., Otto, F. E., Aina, T., Wilson, S., Murphy, J. M., . . . Allen, M. R. (2015, jul). weather@home-development and validation of a very large ensemble modelling system for probabilistic event attribution. *Quarterly Journal of the Royal Meteorological Society, 141*(690), pp. 1528-1545.

McCarthy, M., Christidis, N., Dunstone, N., Fereday, D., Kay, G., Klein-Tank, A., . . . Stott, P. (2019, November 07). Drivers of the UK summer heatwave of 2018. *Weather, 74*, 390-396.

NESDIS. (2018, aug). Record Summer Heat Bakes Europe. *NESDIS*. Retrieved from https://www.nesdis.noaa.gov/content/record-summer-heat-bakes-europe

Press Office. (2018, dec). Chance of summer heatwaves now thirty times more likely. *Met Office News*. Retrieved from https://www.metoffice.gov.uk/about-us/press-office/news/weather-and-climate/2018/2018-uk-summer-heatwave

Publico. (2018, aug). Neuve fallecidos por la ola de calor en Espana. *Publico*. Retrieved from https://www.publico.es/sociedad/nueve-fallecidos-ola-calor-espana.html

Rohde, R., Muller, R. A., Jacobsen, R., Muller, E., Perlmutter, S., Rosenfeld, A., . . . Wickham, C. (2013). A New Estimate of the Average Earth Surface Land Temperature Spanning 1753 to 2011. *Geoinformatics & Geostatistics: An Overview, 1*, p. 1.

Uhe, P., Otto, F. E., Haustein, K., van Oldenborgh, G. J., King, A. D., Wallom, D. C., . . . Cullen, H. (2016, aug). Comparison of methods: Attributing the 2014 record European temperatures to human influences. *Geophysical Research Letters, 43*(16), pp. 8685-8693.

Vautard, R., Gobiet, A., Jacob, D., Belda, M., Colette, A., Déqué, M., . . . Yiou, P. (2013, nov). The simulation of European heat waves from an ensemble of regional climate models within the EURO-CORDEX project. *Climate Dynamics, 41*(9-10), pp. 2555-2575.

Vrac, M., Vaittinada Ayar, P., & Ayar, P. V. (2017, jan). Influence of Bias Correcting Predictors on Statistical Downscaling Models. *Journal of Applied Meteorology and Climatology, 56*(1), pp. 5-26.

Watts, J. (2018, jul). Wildfires rage in Arctic Circle as Sweden calls for help. *The Guardian*. Retrieved from https://www.theguardian.com/world/2018/jul/18/sweden-calls-for-help-as-arctic-circle-hit-by-wildfires

World Weather Attribution. (2018, jul). Heatwave in northern Europe, summer 2018. *worldweatherattribution.org*. Retrieved from

https://www.worldweatherattribution.org/attribution-of-the-2018-heat-in-northern-europe/

Figure Captions

Figure 1: Probability ratios for the 2018 summer heat-event derived from HadGEM3-A factual-counterfactual simulations. Panels a-c show map of increased likelihood in the real world at gridbox scale for the three event timescales analysed respectively. Note that the upper limit on the color scale is 1000 and gridboxes with an infinite probability ratio are shown in dark red. Panel d shows the regional probability ratios for the three timescales; the crosses denote the best-estimate, and the bars denote the 5th-95th percentiles. Note that the best-estimate probability ratios for TM1x in Scandinavia and the Iberian Peninsula were infinite and 2000 respectively.

Figure 2: Panels a-c, probability density functions of the three temporal scales of event statistic for the British Isles, showing HadGEM3-A ACT (factual) and NAT (counterfactual) simulations, and observations from E-OBS; all as anomalies above the model or observed 1961:1990 mean climatology. Thick black lines show the 2018 event defined probabilistically as the HadGEM3-A Historical temperature threshold corresponding to the E-OBS return period, dotted black lines show the event defined in terms of the magnitude observed directly from E-OBS. Panel d, periodograms of JJA daily mean temperature in the British Isles (seasonality and mean removed) calculated as the mean of intraseasonal periodograms for all available years. The HadGEM3-A power spectrum is calculated from the Historical ensemble.

Figures

Figure 1: Probability ratios for the 2018 summer heat-event derived from HadGEM3-A factual-counterfactual simulations. Panels a-c show map of increased likelihood in the real world at gridbox scale for the three event timescales analysed respectively. Note that the upper limit on the color scale is 1000 and gridboxes with an infinite probability ratio are shown in dark red. Panel d shows the regional probability ratios for the three timescales; the crosses denote the best-estimate, and the bars denote the 5th-95th percentiles. Note that the best-estimate probability ratios for TM1x in Scandinavia and the Iberian Peninsula were infinite and 2000 respectively.

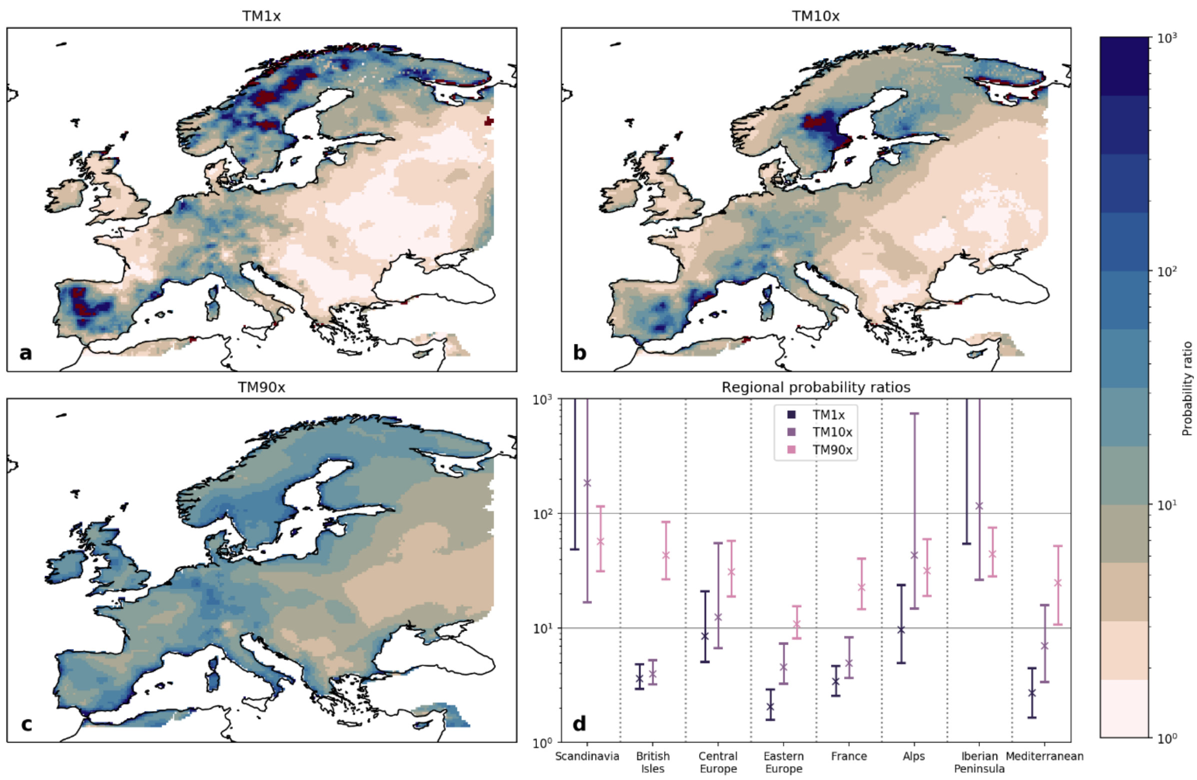

Figure 2: Panels a-c, probability density functions of the three temporal scales of event statistic for the British Isles, showing HadGEM3-A ACT (factual) and NAT (counterfactual) simulations, and observations from E-OBS; all as anomalies above the model or observed 1961:1990 mean climatology. Thick black lines show the 2018 event defined probabilistically as the HadGEM3-A Historical temperature threshold corresponding to the E-OBS return period, dotted black lines show the event defined in terms of the magnitude observed directly from E-OBS. Panel d, periodograms of JJA daily mean temperature in the British Isles (seasonality and mean removed) calculated as the mean of intraseasonal periodograms for all available years. The HadGEM3-A power spectrum is calculated from the Historical ensemble.